Island rule and bone metabolism in fossil murines from Timor

Justyna J. Miszkiewicz[1*], Julien Louys[2], Robin M. D. Beck[3], Patrick Mahoney[4], Ken Aplin[**], Sue O'Connor[5,6]

[1]School of Archaeology and Anthropology, College of Arts and Social Sciences, Australian National University, 0200 Canberra, Australian Capital Territory, Australia

[2]Australian Research Centre for Human Evolution, Environmental Futures Research Institute, Griffith University, 4111 Brisbane, Queensland, Australia

[3]School of Environment and Life Sciences, University of Salford, Salford M5 4WX, United Kingdom

[4]School of Anthropology and Conservation, University of Kent, Canterbury CT2 7NR, United Kingdom

[5]Archaeology and Natural History, College of Asia and the Pacific, Australian National University, 0200 Canberra, Australian Capital Territory, Australia

[6]ARC Centre of Excellence for Australian Biodiversity and Heritage, Australian National University, 0200 Canberra, Australian Capital Territory, Australia

[*]Corresponding author. E-mail: Justyna.Miszkiewicz@anu.edu.au
[**]Deceased

Running title: **Island rule and fossil murine bone metabolism**

ABSTRACT

Skeletal growth rates reconstructed from bone histology in extinct insular hippopotamids, elephants, bovids, and sauropods have been used to infer dwarfism as a response to island conditions. Limited published records of osteocyte lacunae densities (Ot.Dn), a proxy for living osteocyte proliferation, have suggested a slower rate of bone metabolism in giant mammals. Here, we test whether insularity may have affected bone metabolism in a series of small to giant murine rodents from Timor. Ten adult femora were selected from a fossil assemblage dated to the Late Quaternary (ca. 5–18 ka). Femur morphometric data were used in computing phylogenetically-informed body mass regressions, although phylogenetic signal was very low (Pagel's lambda = 0.03). Weight estimates calculated from these femora ranged from 75g to 1188g. Osteocyte lacunae densities from midshaft femur histological sections were evaluated against bone size and estimated body weight. Statistically significant ($p < 0.05$) and strongly negative relationships between Ot.Dn, femur size, and estimated weight were found. Larger specimens were characterised by lower Ot.Dn, indicating that giant murines from Timor may have had a relatively slow pace of bone metabolic activity, consistent with predictions made by the island rule.

Keywords: bone histology, gigantism, insularity, Murinae, osteocyte lacunae, Late Pleistocene, Late Quaternary

INTRODUCTION

Island ecology and biogeography have long served as models for investigating species richness, extinction, speciation, conservation and evolutionary biology (Brown & Kodric-Brown, 1977; Whittaker & Fernández-Palacios, 2007; Sax & Gaines, 2008; MacArthur & Wilson, 2016). Islands are ideal examples of isolated ecosystems that can trigger similar behavioural and biological responses across different animals (Whittaker & Fernández-Palacios, 2007; Miller & Spoolman, 2011; MacArthur & Wilson, 2016). Foster (1964) was the first to discuss body size shifts in species affected by insularity. Van Valen (1973) formalised this under the island rule, which is now known as one of the most fundamental theories in evolutionary biology (Clegg & Owens, 2002; Schillaci *et al.* 2009; Benton *et al.* 2010). It posits that large and small insular mammals decrease and increase their body size, respectively, to accommodate resource availability and drive optimal life histories. Sondaar (1977) then provided a broader perspective on mammal insularity and diversification, highlighting the need to consider islands based on their "oceanic and continental" (p. 617) origin, but study each one within its own context due to complex island histories. Lomolino's (1985, Lomolino *et al.* 2013) later re-examination and re-definition of the island rule specifically encompassed a dwarfism – gigantism gradient (see Lokatis & Jeschke, 2018 for review). Some issues relating to biological constraints limiting a species' plasticity (Meiri *et al.* 2004; 2008), otherwise known as phylogenetic inertia (Darwin, 1859), have since also been considered.

Inferring the cause of body size change in relation to insularity has been subject to much discussion (e.g. Lomolino, 1985; 2013; Millien & Damuth, 2004; Meiri *et al.* 2004; 2006; Itescu *et al.* 2014; Faurby & Svenning, 2016). Trends in body size changes on islands are often

associated with data scatter, likely representing multiple factors contributing to an animal's body mass. These include inter-island differences in competition for resources and mating opportunities, resource availability, geographical factors such as island size and distance from other islands or the mainland, latitude, and climate (McNab, 1971; 2010). In cases of adaptive radiation from a single ancestor, it is also possible for organisms to rapidly diversify into both giant and small forms. Only in conditions of ecological release and time in isolation could body mass trend lines be fitted perfectly (Lomolino, 2005).

When applying the island rule to birds and mammals, which have high resource requirements associated with high metabolic rates compared to other terrestrial vertebrates, body mass is a good indicator of life history and energetic investment (McNab, 2019). Body mass closely reflects basal metabolic rate (BMR) in endotherms, which generate and regulate heat internally to satisfy energetic demands that are required for survival and reproduction (McNab, 2019). Body mass measures, including estimates from fossil material, and large scale meta-analyses have demonstrated gigantism and dwarfism in multiple species globally (Yabe, 1994; Boback & Guyer, 2003; Lomolino 2005; Palombo, 2007; Köhler & Moyà-Solà, 2009; van der Geer *et al.*, 2013). Histology techniques in particular have also proven valuable in reconstructing metabolic activity of the once living bone tissues of different species and taxa by capturing cell metabolic activity indicators preserved in their fossils (e.g. Köhler & Moyà-Solà, 2009; Benton *et al.* 2010; Orlandi-Oliveras *et al.* 2016).

The island rule and rodents

Island rodents, particularly mice, rats, and related species (superfamily Muroidea) have been of particular interest for addressing physiological, morphological, and behavioural responses

to island ecology (Adler & Levins, 1994; Renaud & Millien, 2001; Abdelkrim *et al.* 2005; Harper *et al.* 2005; Towns *et al.*, 2006; Firmat *et al.* 2010; Moncunill-Solé *et al.* 2014; Swift *et al.* 2018; van der Geer, 2018; Geffen & Yom-Tov, 2019). Because of their relatively short lifespans, high level of reproduction, and multiple adaptive radiations, they are important models for studying animal environmental plasticity (Miszkiewicz *et al.* 2019; van der Geer 2019). Comparisons between insular and mainland rodent populations have focused on reproductive behaviour (Stamps & Buechner, 1985) and morphology (Lomolino, 1984), collectively termed the "island syndrome" (Adler & Levins, 1994; Adler, 1996; Russell *et al.* 2011). Isolated insular rodent populations experience a demographic increase in density and dispersal, improved survival and associated reproduction rates, minimised inter-specific competition, and an increase in body mass the more isolated and smaller the island (Foster, 1964). However, there have also been cases of insular rodents that evolved into dwarfed forms (e.g. *Perognathus* spp. on islands bordering Mexico) due to food supply limitations in heterogeneous environments (Lawlor, 1982; Durst & Roth, 2015). Adaptive shifts in rodent morphology and/or behaviour are short or long term depending on the time scale, sample, and context investigated (Palkovacs, 2003). Rodent size adaptation probably occurs initially as a short-term phenotypic change in response to increased island population density. Longer time scale natural selection favouring increased body size would follow when mortality rates and predation are stable and low, as they are on islands (Brown & Sibly, 2006).

Foster's (1964) report of insular mammal gigantism was based on observations of two species of deer mice (*Peromyscus maniculatus* and *P. sitkensis*) of the Queen Charlotte Islands in Canada. Almost double the size of *P. maniculatus, P. sitkensis* was found on the outer small and dispersed islands. Foster (1964) suggested a depauperate fauna, reduced competition for

resources, and minimised predation on small islands favoured insular gigantism as a selective advantage. Empirical evidence for rodent body mass change has since been reported for several other species spanning many geographical locations (e.g. Ventura & Fuster, 2000; Michaux *et al.* 2002; Millien & Damuth, 2004; Russell *et al.* 2011; Pergams *et al.* 2015). Body size increase on small islands has been observed in Japanese *Apodemus speciosus* (Millien & Damuth, 2004), black rats (*Rattus rattus*) in the Mozambique Channel (Russell *et al.* 2011), Polynesian rat *R. exulans* and black rat *R. rattus* in New Zealand and the Pacific islands (Yom-Tov *et al.* 1999), Californian *R. rattus* from Anacapa Island (Pergams *et al.* 2015), woodmouse (*Apodemus sylvaticus*) in the Western Mediterranean Sea (Michaux *et al.* 2002), and *R. rattus* from Congreso Island in Spain (Ventura & Foster, 2000). Skeletal biology literature of island fossil rats mostly reports gross anatomy and morphometric data used for taxonomic purposes. Measurements of dental material (Millien & Damuth, 2004; Louys *et al.* 2018), and cranial and post-cranial morphology (Bocherens *et al.* 2006; Aplin & Helgen, 2010) have been used in taxonomic assignments, but these data have proven equally informative about locomotion, diet, and ecology of rodents such as the case of a now well-studied extinct giant genus *Mikrotia* from the Gargano peninsula (Zafonte and Masini, 1992; Parra *et al.* 1999; Moncunill-Solé *et al.* 2018). Very large, insular members of the murid subfamily Murinae have been reported from the fossil record at multiple locations throughout the world, including the Flores giant rat (*Papagomys armandvillei*) in Indonesia (Locatelli *et al.* 2012), *Coryphomys* from Timor (Aplin & Helgen, 2010), the Tenerife giant rat (*Canariomys bravoi*) from the Canary Islands (Bocherens *et al.* 2006; Firmat *et al.*, 2011). *Megalomys* is a member of another muroid family, Cricetidae, and is known from five very large species from the West Indies (van den Hoek Ostende *et al.* 2017). Some extant giant muroid species that had colonised their islands in the Late Pleistocene or earlier include *Diplothrix legata*, *Apodemus speciosus* and *Apodemus*

argenteus in Japan (Kawamura, 1991), *Phloeomys cumingi* and *P. pallidus* in the Philippines (Rickart & Heaney, 2002), and *Hypogeomys antimena* in Madagascar (Sommer *et al.* 2002).

Bone histology and insular fossil animals

Histological sectioning of fossil bone has proven successful for the reconstruction of tetrapod palaeobiology (Chinsamy-Turan, 2011; de Ricqlès, 2011). By studying microscopic structures and composition in bone samples of fossil vertebrates, skeletal maturation, seasonality, behaviour, and bone metabolism can be reconstructed (Chinsamy-Turan, 2011; Köhler *et al.* 2012). As bone tissue forms, matures, and remodels throughout an animal's lifespan, this information is reflected in the density, organisation, morphology, and geometric properties of bone microstructure (Enlow & Brown, 1956; 1957; 1958). This approach has been successfully applied in insularity contexts (see Kolb *et al.* 2015 for review). For example, slow bone growth rates indicate delayed maturity and extended lifespans in the Late Pleistocene dwarfed Balearic island "goat" (*Myotragus balearicus)* (Köhler, 2010; Köhler & Moyà-Solà, 2009), and insular dwarfism in the Late Jurassic sauropod *Europasaurus holgeri* (Sander *et al.* 2006). To the best of our knowledge, quantitative palaeohistological analyses in relation to island ecology have not been performed for island fossil rodents. Prior research in extinct giant rodent cases reported bone tissue only in the Late Miocene murine *Mikrotia magna* from Gargano Island in Italy (Kolb *et al.*, 2015). We also recently (Miszkiewicz *et al.* 2019) reported descriptions of bone remodeling in one of the giant murines (ANU TDS 0-30 #4) in comparison to a small murine femur (ANU TDD 1 #11) from the same assemblage analysed in the present research. Orlandi-Oliveras et al (2016) observed bone histology of the fossil giant dormouse *Hypnomys onicensis* (Gliridae) from the Balearic Islands indicating increased lifespan that may have been a result of gigantism. While these previous studies have included the description of bone tissue

types and their organisation, the quantification of osteocyte lacunae within the bone matrix in relation to insularity remains to be tested.

Prior research exploring osteocyte lacunae densities (Ot.Dn) has revealed relationships between this measure of bone metabolic activity and negative relationships with body in non-insular settings that may be ultimately linked to aspects of life history. Inter-specific studies of fast maturing and small-bodied, and slow maturing and large-bodied mammal species, exhibit higher and lower osteocyte densities, respectively (Mullender *et al.* 1996; Bromage *et al.* 2009). This phenomenon may reflect an underlying complex relationship between bone ontogeny, rates of metabolism and cell proliferation that are related to body mass (Bromage *et al.* 2009). For example, Ot.Dn decreased with increased body size when compared across selected non-primate mammalian species (Mullender *et al.* 1996). Bromage et al (2009: 393) reported an average of 58,148/mm^3 osteocytes in three females of *R. norvegicus* that had an average body weight of 300 g. In contrast, a hippo (*Hippopotamus amphibius*) with a body weight of 2000 kg, exhibited 16,667/mm^3 osteocytes (Bromage *et al.*, 2009: 393). Furthermore, experimental findings suggest a relationship whereby bone and energy homeostasis is regulated through hormones that are involved both in bone cell biology and body mass accrual (Hogg *et al.*, 2017; see their Figure 11.1). Taken together, these studies suggest a strong inter-specific relationship between Ot.Dn and body size in mammals. This relationship offers therefore a unique way to investigate the growth of fossil rats from island settings.

Hypothesis and prediction

The goal of this study was to evaluate the island rule using Timorese fossil murine rodents whose body size would have ranged from small to giant, as inferred from their bone size. We

studied osteocyte lacunae preserved in femoral midshaft samples to determine if bone metabolic activity, indicative of tissue growth and related to life history, is related with body size among insular members of the rodent subfamily Murinae. We predicted that larger bodied fossil specimens would have a slower rate of osteocyte proliferation compared to those with a smaller body.

MATERIALS AND METHODS

Samples

We examined specimens that represent multiple species in the rodent subfamily Murinae from naturally accumulated late Quaternary fossil deposits of Matja Kuru TD on Timor Island. Timor Island is located in eastern Wallacea, a region compromised of over 17,000 islands. Having never been connected to Southeast Asia (SEA) or Australia, these islands represent permanently isolated geographical regions. Fossil material from this assemblage date to a minimum of ca. 5–18 ka (Louys *et al.* 2017). It was impossible to positively identify the murine species from postcranial elements, so we could not assign them to species or genus. Murine fossil material from Timor includes representatives of four giant extinct genera, of which only *Coryphomys* has been formally described with two species currently recognised, *C. buehleri* and *C. musseri* (Schaub 1937; Aplin and Helgen 2010). We have no way of estimating the potential sex of our specimens, so we cannot exclude sexual dimorphism as a confounding factor in our analyses. However, we note that previous research indicates it to be insignificant in small mammals (e.g. Lu *et al.* 2014). Giant murines have been on the island since at least the Middle Pleistocene (Louys *et al.* 2017), and likely constituted part of human diet until their extinction (Glover, 1971).

The ten specimens represented nine right femora and one left femur (**Figure 1**). The specimens and associated thin sections are housed at the Department of Archaeology and Natural History, and the School of Archaeology and Anthropology at the Australian National University (Canberra, Australia) (see **Tables 1, 2** for accession numbers). For sampling consistency, the femora were selected based on preservation, side, midshaft completeness for thin-sectioning, and ensuring the final sample reflected a range of sizes. Bone histology and midshaft measurements for two of the specimens (TDS0-30#4 and TDD1#11) have been previously reported (Miszkiewicz *et al.* 2019). Most specimens were considered adult as indicated by epiphyseal fusion and mature femoral form. However, some distal and proximal femoral ends were fragmented. We also acknowledge that epiphyseal plate fusion in mammals cannot be entirely relied on for age estimation (Geiger *et al.* 2014). Therefore, we supplemented the age estimates from bone morphology with identification of adult tissue in bone microscopic organisation. For the small specimens, bone histology was very similar to that of adult Wistar rat (*Rattus norvegicus*) femoral cortex (see Singh & Gunberg, 1971; Martiniaková *et al.* 2005; Sengupta, 2013; Miszkiewicz *et al.* 2019). One of the giant femora (TDS0-30#4) also showed evidence of adult Haversian tissue (Miszkiewicz *et al.*, 2019).

Femoral measurements

We quantitatively describe the size of each femur and compare them to a series of Asia-Pacific rodent species of known weight (**Table 2**). Two variables could be consistently applied across the specimens: femur midshaft width in a medial-lateral plane (MLW), and femur midshaft depth in a cranial-caudal (CCD) plane (in mm). These were taken using standard digital callipers (Mitutoyo®). The midshaft was either identified by dividing the length of intact femora in half, or by locating shaft segments immediately distal to the third trochanter (dashed

line in **Figure 1A**). We report maximum length and femoral head diameter where possible (**Table 1**), but exclude them from the statistical analyses as they represent only a fraction of our sample size. We computed body mass estimates using the femoral midshaft measurements. Because this assemblage was commingled and only isolated dental remains were uncovered, a confident match between postcranial and cranial elements per individual is not possible. In addition to the fragmentation of the femora, this meant that we were unable to apply published body mass estimation methods as they include dental data or they do not consider midshaft diameters only as proxies (e.g. Moncunill-Solé *et al.* 2014). Furthermore, as our material is of SEA origin, it warranted the calculation of new, region specific new body mass regression equations based on our new data.

Thin section preparation and bone histology imaging

Standard histological methods for fossil bone were followed to produce thin sections from each femoral midshaft (Chinsamy & Raath, 1992; Miszkiewicz *et al.* 2019). Femora were embedded in Buehler® epoxy resin and cut at midshaft in a transverse plane using a Kemet MICRACUT® 151 Precision Cutter with a diamond cutting blade. Samples were then glued to microscope slides using Araldite®, ground and polished on a series of pads and cloths, dehydrated in ethanol (95% and 100%) baths, cleared in xylene, and cover slipped using a DPX mounting medium. The resulting sections were approximately 100-150 μm thick.

Micro-anatomical descriptions indicate that rat compact bone is mostly avascular, marked with radial canals, osteocytes residing within osteocyte lacunae (Martiniaková *et al.* 2005; Oršolić *et al.* 2018). Haversian, remodelled, tissue in murine bone has been reported only in a few case studies (Kolb *et al.* 2015; Miszkiewicz *et al.* 2019). As osteocytes are responsible for bone

maintenance, they essentially sustain living tissue by signalling mechanical load and facilitating the exchange of nutrients (Han *et al.* 2004; Tate *et al.* 2004). Osteocytes are the most abundant bone cell found in vertebrates (Hall, 2015), and as much as the cells themselves do not typically preserve in fossil bone, the cavities they would have resided in do. Osteocyte lacunae in fossil or archaeological bone can thus be studied as a proxy for osteocyte proliferation and bone metabolism (Bromage *et al.* 2009; Hogg *et al.* 2017; Miszkiewicz, 2016; Miszkiewicz & Mahoney, 2017). We accessed these micro-features from each thin section using standard light microscopy (Olympus BX51 and BX53 microscope with a DP73 and DP74 camera respectively) and analysed them in ImageJ® (1.51k 2013).

All sections were first imaged at a 40x total magnification (~6.07 mm^2 each image) so that an overview micrograph for each sample could be produced. For the larger femoral sections, an average of 10-14 individual images were collected, whereas the smaller femora were easily reproduced from two to three individual images. Each of these were stitched manually in Adobe Photoshop CC 2014 to create a starting point from which to identify the best preserved and taphonomy/bio-erosion free region of interest (ROI). Unlike modern or fresh bone, the palaeontological context of our samples meant that there was incomplete and inconsistent preservation of microstructure. Therefore, the selection of ROIs for data collection was determined by the visibility of, and our confidence in identifying, osteocyte lacunae. Where possible, we selected the same anatomical aspect of each femur so that osteocyte lacunae data could be compared consistently across the whole sample. This resulted in isolating the lateral femur region with some caudal or cranial overlap (**Figure 1B**). Ultimately, we captured osteocyte lacunae data from one ROI per section at 100x total magnification representing an image that measures ~0.93 mm^2. The bone area within each image ranged from ~0.93 mm^2 in

the giant rats to ~0.35 mm^2 in the smaller rats. In the latter case, the area of the bone itself was measured by directly tracing the bone tissue, excluding image regions that were empty. Using the MultiPoint tool in ImageJ® (1.51k 2013), osteocyte lacunae were first recorded as total counts from the most superior surface of each section. Prior to counting, all images were adjusted to grey scale (black and white intensity = 100) and then exposed (offset = -0.100) in Adobe Photoshop CC 2014 to enhance each lacuna so that they could be distinguished against the white background (**Figure 1B**). In order to estimate densities, a standard Ot.Dn (osteocyte lacunae density = osteocyte lacunae count/ section area in mm^2) variable was created by dividing each osteocyte lacunae count by the bone area examined in mm^2 (Li *et al.* 2011; Miszkiewicz, 2016). To check for potential observer bias, osteocyte lacunae in two randomly selected images from our image bank were independently scored by three observers – two authors of the present study (JM, JL), and one external histologist (TJ Stewart).

Statistical analyses

All statistical analyses were conducted in IBM SPSS Statistics 22.0 (2013), Past3 (Hammer *et al.*, 2001), and R 3.6.0. We split the analyses into two steps – 1) testing for a phylogenetic signal and creating body mass regressions, 2) assessing relationships between measures of body size and Ot.Dn by examining linear trends and testing for allometric changes (Kilmer & Rodríguez, 2017). As we only had three independent data points, inter-observer measurements were compared between the repeated data descriptively by assessing the extent of deviation from the mean. The measurements were deemed repeatable if the disagreement was < 0.05%.

1) Phylogenetic signal and body mass regressions

To produce a body mass regression equation that could be used to estimate body mass for our Timorese specimens, we collected CCD and MLW measurements for specimens of known body mass for 17 Asia-Pacific murine species (**Table 2**). Where data were available for multiple specimens of the same species, these were combined to produce mean estimates for that species (**Table 2**). The final CCD and MLW measurements and body mass for each species were natural-logged (ln) transformed prior to analysis. We used a phylogenetic generalised least squares (PGLS) approach (Symonds & Blomberg, 2014), with uncertainty in phylogenetic relationships and divergence times among our species taken into account using the R package sensiPhy (Paterno *et al.* 2018) and 1000 trees from the "Phylacine" database (Faurby *et al.* 2018), pruned to match our set of 17 species using the "keep.tip" function of the R package ape (Paradis & Schliep, 2019). We used the "physig" function of sensiPhy to calculate the maximum likelihood estimate of Pagel's lambda (λ) in the residuals of our data as a measure of phylogenetic signal, and then used this value of λ to determine the best-fitting regression. We calculated three different regressions, using body mass and either: 1) CCD, 2) MLW, or 3) cross-sectional area of the femoral midshaft, which we calculated as π x (0.5 x CCD) x (0.5 x MLW), i.e., treating it as an ellipse. We then used the Akaike Information Criterion (AIC) to determine which of these three regressions showed the best fit to our data, and used the best-fitting regression to estimate body mass for our Timorese specimens.

2) Evaluating relationships between femur size, body mass, and osteocyte lacunae

Firstly, all the raw data for body mass estimates (g), CCD (mm), MLW (mm), and Ot.Dn were correlated using non-parametric Spearman's *Rho* tests to assess linear agreements between data. These were repeated on the raw Ot.Dn data corrected by femur midshaft size

(Ot.Dn/MLW and Ot.Dn/CCD). The results from these correlations were interpreted following Taylor (1990), whereby *Rho* > 0.67 is considered a high or strong correlation. To assess allometric changes in Ot.Dn along with femur size and body mass estimates we used ordinary least squares regressions (OLS) on log10 transformed data (which decreased data variability). We interpret the r^2, slope (*b*), confidence interval (CI), intercept (*Y*), and statistical significance of these models using uncorrected *p* as well as Bonferroni corrected (uncorrected *p* divided by the number of repeated tests), more conservative, *p* for each set of analysis. Plots fitting OLS regressions illustrate the trend line and CIs to visually describe the scatter of data.

RESULTS

There was no inter-observer error in the independent measurements, with the three observers providing almost equal counts of lacunae per image (image 1 mean 127.33, SD 2.08, similarity = 98.37%; image 2 mean 132.67, SD = 2.52, similarity = 98.10%). The largest midshaft femur measured 7.25 mm in MLW and 5.89 mm in CCD, respectively (**Tables 1-3**). The smallest examined femur was of 2.33 mm MLW and 1.98 mm CCD, respectively (Miszkiewicz *et al.*, 2019). Body mass estimates for the sample ranged from 75g in the smallest specimen to 1188g in the largest specimen. We incorporated these estimates (relying on MLW and CCD data) into a bar chart encompassing modern rat data of known weight (**Figure 2, Table 2**). This shows that the smaller fossil murines were likely similar in their body mass to a house mouse (*Mus domesticus*), whereas the giant murines may have been comparable to a subalpine woolly rat (*Mallomys istapantap*, up to 2 kg in weight).

Body mass estimates

The phylogenetic signal (measured by Pagel's lambda) in our data for specimens of known body mass for 17 Asia-Pacific species (**Table 2**) was very low and non-significant (mean = 0.03, CI = 0.02, CI = 0.04, $p = 0.99$). AIC values for our three regressions were as follows: ln(MLWfemur width) = 10.38, ln(CCDfemur depth) = 16.53, ln(femoral midshaft cross-sectional areafemur area) = 8.59. As lower AIC values represent better model fit, it is clear that combining femur width and depth into an estimate of femur area resulted in a better fitting model. The PGLS regression for ln(femur area) and an the maximum likelihood (ML) estimate of Pagel's lambda ($\lambda = 0.03$) was:

ln(body mass) = 1.24 x ln[(femur area = π x (0.5 x CCD) x (0.5 x MLW)] + 2.724

Body mass estimates for the Timor specimens, based on the above equation, are reported in **Table 2.**

Osteocyte lacunae densities

Osteocyte lacunae density data ranged from 2483.21/mm^2 minimum to 3936.32/mm^2 maximum. However, corrections by femur size adjusted the data to 342.51/mm^2 and 1499.30/mm^2 range in the MLW category, and 421.60/mm^2 to 1764.32/mm^2 in the CCD measure of femur shaft (**Tables 1-3**). The results of Spearman's *Rho* tests (**Table 4**) suggest that Ot.Dn data are in strongly negative and statistically significant relationships with measures of femur size and body mass estimates. The *Rho* achieved in these cases was -0.952 to -0.661 with $p < 0.05$. However, when CCD was considered, these relationships were not consistent, whereby *Rho* was -0.576 ($p = 0.082$) when raw Ot.Dn were included in the analysis. When using a more conservative Bonferroni correction on repeated tests, the correlation between

estimated body mass, and MLW and raw Ot.Dn did not meet significance, with $p = 0.038$ and 0.019 respectively.

Ordinary least squares regression of all log transformed data resulted in an almost consistently statistically significant and strong models that showed negative allometry (**Table 4**). Two of the models - log(estimated body mass), log(CCD), and log(Ot.Dn), returned $p > 0.05$ and had weak r^2. However, most of the models were statistically significant at $\alpha = 0.05$, except for Bonferroni corrected log(MLW) and log(Ot.Dn) where $0.05 > p > 0.017$. The data scatter around regression lines was wider in the cases where raw data are used, but better fitting models can be seen for those where the size of the femur is accounted for in Ot.Dn (**Figure 3**).

DISCUSSION

Our analyses revealed statistically significant negative correlations, and an allometric relationship between the histological and macroscopic measures of bone metabolism and body mass in a range of giant and small fossil murine rodents from Timor Island. Collectively, these provide clear evidence that fossil murine gigantism was associated with a slowing down of bone metabolism as inferred from low osteocyte lacunae densities. In contrast, the smaller murines in our sample exhibit increased osteocyte lacunae densities, indicating accelerated bone metabolism. Our study has implications for current understanding of the evolution of mammalian bone physiology in relation to body mass and insularity, as well as the palaeoenvironments of Timor.

Bone metabolism

This study unlocks bone physiology from cell structures preserved in thin sections of fossil femora to understand the biological adaptation of Timorese island members of the rodent subfamily Murinae, and to examine the relationships between bone osteocyte lacunae densities and body mass when compared between these in mammalian species. We have previously shown changes in osteocyte lacunae densities can be linked to bone remodelling rates (e.g. Miszkiewicz, 2016), and as such can provide insights into bone metabolism fluctuations. When examined within living mammals, strong inverse correlations between Ot.Dn and body mass show that osteocyte proliferation corresponds to body mass (Hogg *et al.* 2017). Data presented here support these ideas as they demonstrate a strongly negative decline in Ot.Dn with increasing within Timorese island murines. These data are similar to previous inter-specific findings for extant non-primate mammals (Mullender *et al.* 1996), and to those described by Bromage et al (2009) for species that included adult pygmy (*Phanourios minutus*) and common hippo (*Hippopotamus amphibious*), as well as the Mohol bushbaby (lesser galagos, *Galago moholi*) and greater dwarf lemur (*Cheirogales major*) (Bromage *et al.*, 2009: 393). A pygmy hippo of an approximate 200 kg body mass had an average Ot.Dn reported as 23,641/mm^3, whereas its larger counterpart (*H. amphibius*) had an Ot.Dn of 16,667/mm^3. In the same study, an adult lesser galago with an approximate 244 g weight had 51,724/mm^3 Ot.Dn, which was much higher than the 31,526/mm^3 Ot.Dn from a greater galago with a body weight of 400 g. Our data conform to this general pattern. Our study shows a much more widely dispersed osteocyte lacunae in the giant murine specimen when compared to its smaller counterpart (**Figure 1C**), and body size and Ot.Dn are related through negative allometry.

Bone histology limitations of our study pertain to being understood two-dimensionally only, whereas three-dimensional scans of each entire femur in the sample may yield more osteocyte lacunae data in the future. We are also unable to make further connections to energy variables, such as the BMR, because of the nature of the samples. With no direct measures of muscle or physical activity in our fossil murine sample, we are limited in understanding how their energetic expenditure and heat generation may have fitted into life history strategies (McNab, 2019). Finally, the unknown species identification limited our interpretations of the Ot.Dn links with phylogeny. However, previous accounts of inter-specific variation in bone micro-organisation have cited animal size and lifespan as more direct influences on histology than phylogeny (de Ricqlès, 1993; Greenlee & Dunnell, 2010).

The extinct giant murines of Timor

As predicted by the island rule, animals may change with response to insular environments due to selective pressures that encourage anatomical and behavioural modifications. Smaller, lighter, and faster growing mammals can adapt more easily than those that have increased energetic demands. While being smaller comes with many advantages, it also decreases longevity as outlined in the classic r and K-selection evolutionary strategy principles (Pianka, 1970). The relatively slow bone metabolism of giant Timorese murines could indicate extended lifespans, which can be linked to favourable palaeoenvironments.

It is extremely difficult to pinpoint specific casualty of our giant murine extinction as multiple factors must have played a role in their demise. However, when compared to prior palaeobiological models that test extinction causality in small mammals in islands (e.g. Bover & Alcover, 2008), we can at least propose some environmental extinction elements. For

example, Bover and Alcover (2008) examined the extinction of Mallorcan small mammals analysing climate, predation, competition, habitat loss/ modification, and anthropogenic factors as potential reasons driving extinction in the Western Mediterranean. The authors obtained radiocarbon ages from fossil bone collagen to reconstruct uncertainty and restricted periods of extinction for species of Balearic dormouse (*Eliomys morpheus*) and the Balearic shrew (*Asoriculus hidalgo*), and corroborated archaeological and direct dating data of introduced garden dormouse *Eliomys quercinus* and the wood mouse *Apodemus sylvaticus*. They concluded that the extinction of the Mallorcan small mammals would have been most likely indirectly caused by human activity (the spread of disease). For the giant murines of Timor, we can find supporting evidence in the historical and archaeological record for at least two of these items – human co-existence with giant murines, and habitat modification on the island of Timor.

Fossil evidence suggests that giant murines were in Timor from the Middle Pleistocene (Louys *et al.* 2017), by which time the island was also home to small-bodied stegodons (*Stegodon `trigonocephalus'* and *Stegodon timorensis*) - elephant-like animals that may have evolved into pygmy forms on the island (Louys *et al.* 2016). This hints at the effect of insularity impacting more than one mammal in Timor. To that end, giant murines have been found in association with humans in Timor for more than 40,000 years (Hawkins *et al.* 2017). Glover (1971:177), when reviewing archaeological and palaeontological excavations on the island of Timor since about 1935, noted that giant murines would have been "the principal prey" (in addition to pteropodid bats) of the first human groups. Increasing human contact may have not only entailed predation: it would have also likely led to significant habitat alteration, introduction of competitors, other predators, and disease.

Human driven deforestation in SEA is a well-established issue that contributes to the reduction of resources and elimination forest ecology (see McWilliam, 2005; O'Connor *et al.* 2012). Modern biodiversity conservation efforts have continually documented the disappearance of rich native habitats in areas densely populated and exploited by humans in SEA (Sodhi *et al.* 2010; Hughes, 2017; Carlson *et al.* 2018). Historical annotations indicate that Timor became an important centre for timber export of white sandalwood ca. 1500 AD (McWilliam, 2005; O'Connor *et al.* 2012), with prior introduction of metal tools (bronze and iron) to island SEA sometime 2500 and 1500 years ago (Higham, 1996; Bulbeck, 2008). These tool developments would have facilitated effective slash-and-burn agriculture, with the later timber export activity accelerating forest cultivation. By the Timorese fort building period, ~1500 years ago, many small, but no giant murine fossils are recovered in excavations, suggesting extinction of the latter by this time (O'Connor & Aplin, 2007)..

While more direct evidence for the Timor palaeoenvironments, and a larger sample size, is needed, our histology study suggests that the slower bone metabolism of giant murines fitted principles of gigantism under the island rule. They may have been associated with slower growth and maturation requiring relatively higher amounts of energy obtained from good quality or quantity of resources, low levels of predation, facilitating longevity and increased offspring quality (Reznick *et al.* 2002; Dammhahn *et al.* 2018). Our findings match those from another palaeohistology study that inferred an "exceptionally long lifespan" (Orlandi-Oliveras *et al.* 2016: 238) from bone histology in a giant fossil glirid rodent, *Hypnomys onicensis*, on the Balearic Islands, confirming slower life history in an insular context. We acknowledge that true "gigantism" of our specimens cannot be confirmed until we know the body mass of their

ancestors and have an accurate phylogeny. The island rule specifies that if a colonising ancestral species was initially small, and the newly colonised island marked with favourable habitats, evolving into a giant form would be selectively advantageous. While we know that Timor has never been connected to SEA or Australia, and thus has been truly geographically isolated throughout its history, cases of island rodents that evolved into dwarfed from larger forms following deterioration in food resources are known (Durst & Roth, 2015).

CONCLUSIONS

Lab rats have long been used in biology research, letting us observe animal phenotypic change upon experimental modification of external environmental and internal genotypic conditions. Here, we conducted an experiment in deep time, assessing murine size and bone microanatomy in the context of a changing and insular environment. The gradient of murine size in this sample served as a platform for investigating links between bone metabolism and its response to insularity. We show that the now extinct giant murines of Timor were likely characterised by slow bone metabolism, which could be related to abundant resources and plentiful forests until human driven action destroyed these habitats. This finding is consistent with predictions made from the island rule. We also find that surviving smaller murines were equipped with faster bone metabolism, allowing them to survive less certain environmental contexts once anthropogenic alteration increased. These findings further our understanding of vertebrate bone tissue metabolism, its adaptation in response to ecological change, along with its versatility and plasticity that can be reconstructed at a microscopic level.

ACKNOWLEDGMENTS

Shimona Kealy selected murine specimens for this experiment. Tahlia Stewart participated in the inter-observer error test. Fieldwork in Timor and subsequent analysis of specimens were

undertaken with permissions from the Director General of Culture, Mrs Cecília Assis, Ministry of Tourism, Art and Culture, Timor-Leste. Research funding was received from the Australian Research Council (LF120100156 to O'Connor, FT160100450 to Louys, DE190100068 to Miszkiewicz). We thank three anonymous reviewers, Blanca Moncunill-Solé, and John A. Allen for feedback and constructive suggestions that greatly improved this manuscript. We are grateful to Kristofer Helgen for advice on specimen accessioning. We dedicate this paper to the late Ken Aplin.

REFERENCES

Abdelkrim J, Pascal M, Samadi S. 2005. Island colonization and founder effects: the invasion of the Guadeloupe islands by ship rats (*Rattus rattus*). Mol Ecol 14: 2923-2931.

Adler GH. 1996. The island syndrome in isolated populations of a tropical forest rodent. Oecologia 108: 694-700.

Adler GH, Levins R. 1994. The island syndrome in rodent populations. Q Rev Biol 69: 473-490.

Aplin KP, Helgen KM. 2010. Quaternary murid rodents of Timor Part I: new material of *Coryphomys buehleri* Schaub, 1937, and description of a second species of the genus. Bull Am Mus Nat 341: 1-80.

Benton MJ, Csiki Z, Grigorescu D, Redelstorff R, Sander PM, Stein K, Weishampel D. B. 2010. Dinosaurs and the island rule: The dwarfed dinosaurs from Haţeg Island. Palaeogeogr Palaeoclimatol Palaeoecol 293: 438-454.

Boback SM, Guyer C. 2003. Empirical evidence for an optimal body size in snakes. Evol 57, 345-351.

Bocherens H, Michaux J, Talavera FG, van der Plicht J. 2006. Extinction of endemic vertebrates on islands: the case of the giant rat *Canariomys bravoi* (Mammalia, Rodentia) on Tenerife (Canary Islands, Spain). C R Palevol 5: 885-91.

Bover P, Alcover JA. 2008. Extinction of the autochthonous small mammals of Mallorca (Gymnesic Islands, Western Mediterranean) and its ecological consequences. J Biogeogr 35: 1112-1122.

Bromage TG, Lacruz RS, Hogg R, Goldman HM, McFarlin SC, Warshaw J, Dirks W, Perez-Ochoa A, Smolyar I, Enlow DH, Boyde A. 2009. Lamellar bone is an incremental tissue reconciling enamel rhythms, body size, and organismal life history. Calcif Tissue Int 84: 388-404.

Brown JH, Kodric-Brown A. 1977. Turnover rates in insular biogeography: effect of immigration on extinction. Ecol 58: 445-449.

Brown JH, Sibly RM. 2006. Life-history evolution under a production constraint. Proc Natl Acad Sci 103: 17595-17599.

Bulbeck D. 2008. An integrated perspective on the Austronesian diaspora: The switch from cereal agriculture to maritime foraging in the colonisation of Island Southeast Asia. Aus Archaeol 67: 31-51.

Carlson KM, Heilmayr R, Gibbs HK, Noojipady P, Burns DN, Morton DC, Walker NF, Paoli GD, Kremen C. 2018. Effect of oil palm sustainability certification on deforestation and fire in Indonesia. Proc Natl Acad Sci 115: 121-6.

Chinsamy A, Raath MA. 1992. Preparation of fossil bone for histological examination. Palaeont Afr 29: 39 – 44.

Chinsamy-Turan A. 2011. Forerunners of mammals: radiation, histology, biology. Bloomington, US: Indiana University Press.

Clegg SM, Owens PF. 2002. The 'island rule' in birds: medium body size and its ecological explanation. Proc R Soc Lond B Biol Sci 269: 1359-1365.

Dammhahn M, Dingemanse NJ, Niemelä PT, Réale D. 2018. Pace-of-life syndromes: a framework for the adaptive integration of behaviour, physiology and life history. Behav Ecol Sociobiol 72: 62.

Darwin C. 1859. The Origin of Species by Means of Natural Selection: Or, The Preservation of Favored Races in the Struggle for Life. London, UK: Murray.

de Ricqlès AJ. 1993. Some remarks on palaeohistology from a comparative evolutionary point of view. In: Grupe G, Garland AN, eds: Histology of ancient human bone: methods and diagnosis. Berlin: Springer, 37-77.

de Ricqlès AJ. 2011. Vertebrate palaeohistology: Past and future. C R Palevol 10: 509-515.

Durst PA, Roth VL. 2015. Mainland size variation informs predictive models of exceptional insular body size change in rodents. P Roy Soc B-Biol Sci 282: 20150239.

Enlow DH, Brown SO. 1956. A comparative histological study of fossil and recent bone tissues. Part I. Tex J Sci 8: 405-443.

Enlow DH, Brown SO. 1957. A comparative histological study of fossil and recent bone tissues. Part II. Tex J Sci 9: 186-214.

Enlow DH, Brown SO. 1958. A comparative histological study of fossil and recent bone tissues. Tex J Sci 10: 187-230.

Faurby S, Davis M, Pedersen RO, Schowanek SD, Antonelli A, Svenning JC. 2018. PHYLACINE 1.2: The Phylogenetic atlas of mammal macroecology. Ecology 99: 2626.

Faurby S, Svenning J-C. 2016. Resurrection of the island rule: human-driven extinctions have obscured a basic evolutionary pattern. Am Nat 187: 812–820.

571 Firmat C, Rodrigues HG, Hutterer R, Rando JC, Alcover JA, Michaux J. 2011. Diet of the
572 extinct Lava mouse *Malpaisomys insularis* from the Canary Islands: insights from dental
573 microwear. Naturwiss 98: 33-7.

574 Firmat C, Rodrigues HG, Renaud S, Hutterer R, Garcia-Talavera Fr, Michaux J. 2010.
575 Mandible morphology, dental microwear, and diet of the extinct giant rats *Canariomys*
576 (Rodentia: Murinae) of the Canary Islands (Spain). Biol J Linn Soc 101: 28-40.

577 Foster JB. 1964. Evolution of mammals on islands. Nature 202: 234-235.

578 Geffen E, Yom-Tov Y. 2019. Pacific island invasions: how do settlement time, latitude, island
579 area and number of competitors affect body size of the kiore (Polynesian rat) across the
580 Pacific?. Biol J Linn Soc 126: 462–470.

581 Geiger M, Forasiepi AM, Koyabu D, Sánchez-Villagra MR. 2014. Heterochrony and post-natal
582 growth in mammals–an examination of growth plates in limbs. J Evo Biol 27: 98-115.

583 Glover IC. 1971. Prehistoric research in Timor. In: Mulvaney DJ, Golson J, eds: Aboriginal
584 man and environment in Australia. Canberra: Australian National University Press, 154-181.

585 Greenlee DM, Dunnell RC. 2010. Identification of fragmentary bone from the Pacific. J
586 Archaeol Sci 37: 957-970.

587 Hall BK. 2015. Bones and cartilage: developmental and evolutionary skeletal biology. London,
588 UK: Elsevier Academic Press.

589 Hammer Ø, Harper DAT, Ryan PD. 2001. PAST-palaeontological statistics, ver. 1.89. Palaeont
590 Electr 4: 1–9.

Han Y, Cowin SC, Schaffler MB, Weinbaum S. 2004. Mechanotransduction and strain amplification in osteocyte cell processes. Proc Natl Acad Sci 101: 16689-94.

Harper GA, Dickinson KJ, Seddon PJ. 2005. Habitat use by three rat species (*Rattus* spp.) on Stewart Island/Rakiura, New Zealand. N Z J Ecol 29: 251-260.

Hawkins S, O'Connor S, Maloney TR, Litster M, Kealy S, Fenner JN, Aplin K, Boulanger C, Brockwell S, Willan R, Piotto E. Oldest human occupation of Wallacea at Laili Cave, Timor-Leste, shows broad-spectrum foraging responses to late Pleistocene environments. Quaternary Sci Rev 171: 58-72.

Higham C. 1996. The Bronze Age of Southeast Asia. Cambridge, UK: Cambridge University Press.

Hogg RT, Bromage TG, Goldman HM, Katris JA, Clement JG. 2017. The Havers–Halberg oscillation and bone metabolism. In: Percival CJ, Richtsmeier, JT. Building bones: bone formation and development in anthropology. Cambridge, UK: Cambridge University Press. pp. 254-280.

Hughes AC. 2017. Understanding the drivers of Southeast Asian biodiversity loss. Ecosphere 8: e01624.

Itescu Y, Karraker NE, Raia P, Pritchard PC, Meiri S. 2014. Is the island rule general? Turtles disagree. Glob Ecol Biogeogr 23: 689-700.

Kawamura Y. 1991. Quaternary mammalian faunas in the Japanese Islands. Quaternary Res (Daiyonki-Kenkyu) 30: 213-220.

Kilmer JT, Rodríguez RL. 2017. Ordinary least squares regression is indicated for studies of allometry. J Evol Biol 30: 4-12.

Kolb C, Scheyer TM, Veitschegger K, Forasiepi AM, Amson E, van der Geer AA, van den Hoek Ostende LW, Hayashi S, Sánchez-Villagra MR. 2015. Mammalian bone palaeohistology: a survey and new data with emphasis on island forms. PeerJ 22: e1358.

Köhler M. 2010. Fast or slow? The evolution of life history traits associated with insular dwarfing. In: Pérez-Mellado V, Ramon C, eds: Islands and evolution, Mallorca, Spain: Institut Menorquí d'Estudis Recerca, 261-280.

Köhler M, Marín-Moratalla N, Jordana X, Aanes R. 2012. Seasonal bone growth and physiology in endotherms shed light on dinosaur physiology. Nature 487: 358.

Köhler M, Moyà-Solà S. 2009. Physiological and life history strategies of a fossil large mammal in a resource-limited environment. Proc Natl Acad Sci 106: 20354-20358.

Lawlor TE. 1982. The evolution of body size in mammals: evidence from insular populations in Mexico. Am Nat 119: 54-72.

Li ZC, Jiang SD, Yan J, Jiang LS, Dai LY. 2011. Small-animal PET/CT assessment of bone microdamage in ovariectomized rats. J Nucl Med 52: 769-775.

Locatelli E, Due RA, van den Bergh GD, van den Hoek Ostende LW. 2012. Pleistocene survivors and Holocene extinctions: the giant rats from Liang Bua (Flores, Indonesia). Quat Int 19: 47-57.

Lokatis S, Jeschke JM. 2018. The island rule: An assessment of biases and research trends. J Biogeog 45: 289-303.

Lomolino MV. 1984. Immigrant selection, predation, and the distributions of *Microtus pennsylvanicus* and *Blarina brevicauda* on islands. Am Nat 123, 468-83.

Lomolino MV. 1985. Body size of mammals on islands: the island rule reexamined. Am Nat 125: 310-6.

Lomolino MV. 2005. Body size evolution in insular vertebrates: generality of the island rule. J Biogeogr 32: 1683-1699.

Lomolino MV, van der Geer AA, Lyras GA, Palombo MR, Sax DF, Rozzi R. 2013. Of mice and mammoths: generality and antiquity of the island rule. J Biogeogr 40: 1427-39.

Louys J, Kealy S, O'Connor S, Price GJ, Hawkins S, Aplin K, Rizal Y, Zaim J, Tanudirjo DA, Santoso WD, Hidayah AR. 2017. Differential preservation of vertebrates in Southeast Asian caves. Int J Speleol 46: 379-408.

Louys J, Price GJ, O'Connor S. 2016. Direct dating of Pleistocene stegodon from Timor Island, East Nusa Tenggara. PeerJ 10: e1788.

Louys J, O'Connor S, Mahirta, Higgins P, Hawkins S, Maloney T. 2018. New genus and species of giant rat from Alor Island, Indonesia. J Asia Pac Biodivers 11: 503-510

Lu D, Zhou CQ, Liao WB. 2014. Sexual size dimorphism lacking in small mammals. North-West J Zool 10: 53–59.

MacArthur RH, Wilson EO. 2016. The theory of island biogeography. Princeton, US: Princeton University Press.

Martiniaková M, Grosskopf B, Vondráková M, Omelka R, Fabiš M. 2005. Observation of the microstructure of rat cortical bone tissue. Scripta Med 78: 45-50.

McNab BK. 1971. On the ecological significance of Bergmann's rule. Ecol 52: 845-854.

McNab BK. 2010. Geographic and temporal correlations of mammalian size reconsidered: a resource rule. Oecologia 164: 13-23.

McNab BK. 2019. What determines the basal rate of metabolism?. J Exper Biol, 222: jeb205591.

McWilliam A. 2005. Haumeni, not many: renewed plunder and mismanagement in the Timorese sandalwood industry. Mod Asian Stud 39: 285-320.

Meiri S, Cooper N, Purvis A. 2008. The island rule: made to be broken?. Proc R Soc Lon B Biolo Sci 275: 141-148.

Meiri S, Dayan T, Simberloff D. 2004. Body size of insular carnivores: little support for the island rule. Am Nat 163: 469-479.

Meiri S, Dayan T, Simberloff D. 2006. The generality of the island rule reexamined. J Biogeogr 33: 1571-1577.

Michaux JR, De Bellocq JG, Sarà M, Morand S. 2002. Body size increase in insular rodent populations: a role for predators?. Glob Ecol Biogeog 11: 427-436.

Miller G, Spoolman S. 2011. Living in the environment: principles, connections, and solutions. Belmont, US: Brooks/Cole.

Millien V, Damuth J. 2004. Climate change and size evolution in an island rodent species: new perspectives on the island rule. Evol 58: 1353-1360.

Miszkiewicz JJ. 2016. Investigating histomorphometric relationships at the human femoral midshaft in a biomechanical context. J Bone Miner Metab 34: 179-192.

Miszkiewicz JJ, Louys J, O'Connor S. 2019. Microanatomical record of cortical bone remodeling and high vascularity in a fossil giant rat midshaft femur. Anat Rec 302: 1934-1940.

Miszkiewicz JJ, Mahoney P. 2017. Human bone and dental histology in an archaeological context. In: Thompson T, Errickson D, eds: Human remains: another dimension, London, UK: Elsevier Academic Press, 29-43.

Moncunill- Solé B, Jordana X, Köhler M. 2018. Where did *Mikrotia magna* originate? Drawing ecogeographical inferences from body mass reconstructions. Geobios 51: 359-366.

Moncunill-Solé B, Jordana X, Marín-Moratalla N, Moyà-Solà S, Köhler M. 2014. How large are the extinct giant insular rodents? New body mass estimations from teeth and bones. Integr Zool 9: 197-212.

Mullender MG, Huiskes R, Versleyen H, Buma P. 1996. Osteocyte density and histomorphometric parameters in cancellous bone of the proximal femur in five mammalian species. J Orthop Res 14: 972-979.

O'Connor S, Aplin K. 2007. A matter of balance: An overview of Pleistocene occupation history and the impact of the Last Glacial Phase in East Timor and the Aru Islands, eastern Indonesia. Archaeol Oceania 42: 82-90.

O'Connor S, McWilliam A, Fenner JN, Brockwell S. 2012. Examining the origin of fortifications in East Timor: social and environmental factors. J Isl Coast Archaeol 7: 200-218.

692 Orlandi-Oliveras G, Jordana X, Moncunill-Solé B, Köhler M. 2016. Bone histology of the giant
693 fossil dormouse *Hypnomys onicensis* (Gliridae, Rodentia) from Balearic Islands. C R Palevol
694 15: 238-244.

695 Oršolić N, Jeleč Ž, Nemrava J, Balta V, Gregorović G, Jeleč D. 2018. Effect of quercetin on
696 bone mineral status and markers of bone turnover in retinoic acid-induced osteoporosis. Pol J
697 Food Nutr Sci 68: 149-62.

698 Paradis E, Schliep K. 2019. ape 5.0: an environment for modern phylogenetics and
699 evolutionary analyses in R. Bioinformatics 35: 526-528.

700 Palkovacs EP. 2003. Explaining adaptive shifts in body size on islands: a life history approach.
701 Oikos 103: 37–44

702 Palombo MR. 2007. How can endemic proboscideans help us understand the “island rule”? A
703 case study of Mediterranean islands. Quat Int 169: 105-124.

704 Parra V, Jaeger JJ, Bocherens H. 1999. The skull of *Microtia*, an extinct burrowing murine
705 rodent of the late Neogene Gargano palaeoisland. Lethaia 32: 89-100.

706 Paterno GB, Penone C, Werner GDA. 2018. sensiPhy: An R-package for sensitivity analysis
707 in phylogenetic comparative methods. Methods Ecol Evol 9: 1461-1467.

708 Pergams OR, Byrn D, Lee KL, Jackson R. 2015. Rapid morphological change in black rats
709 (*Rattus rattus*) after an island introduction. PeerJ 3: e812.

710 Pianka ER. 1970. On r-and K-selection. Am Nat 104: 592-597.

Renaud S, Millien V. 2001. Intra-and interspecific morphological variation in the field mouse species *Apodemus argenteus* and *A. speciosus* in the Japanese archipelago: the role of insular isolation and biogeographic gradients. Biol J Linn Soc 74: 557-69.

Reznick D, Bryant MJ, Bashey F. 2002. r-and K-selection revisited: the role of population regulation in life-history evolution. Ecol 83: 1509-20.

Rickart EA, Heaney LR. 2002. Further studies on the chromosomes of Philippine rodents (Muridae: Murinae). Proc Biol Soc Wash 115: 473-487.

Russell JC, Ringler D, Trombini A, Le Corre M. 2011. The island syndrome and population dynamics of introduced rats. Oecologia 167 : 667-76.

Sander PM, Mateus O, Laven T, Knötschke N. 2006. Bone histology indicates insular dwarfism in a new Late Jurassic sauropod dinosaur. Nature 441: 739.

Sax DF, Gaines SD. 2008. Species invasions and extinction: the future of native biodiversity on islands. Proc Natl Acad Sci 105: 11490-11497.

Sengupta P. 2013. The laboratory rat: relating its age with human's. Int J Prevent Med 4: 624–630.

Schaub S. 1937. Ein neuer Muride von Timor. Verhandlungen der Naturforschenden Gesellschaft in Basel 48: 1-6.

Schillaci MA, Meijaard E, Clark T. 2009. The effect of island area on body size in a primate species from the Sunda Shelf Islands. J Biogeogr 36: 362-371.

Singh IJ, Gunberg DL. 1971. Quantitative histology of changes with age in rat bone cortex. J Morphol 133: 241-51.

Sommer S, Volahy AT, Seal US. (2002). A population and habitat viability assessment for the highly endangered giant jumping rat (*Hypogeomys antimena*), the largest extant endemic rodent of Madagascar. Anim Conserv 5: 263-273.

Sodhi NS, Posa MR, Lee TM, Bickford D, Koh LP, Brook BW. 2010. The state and conservation of Southeast Asian biodiversity. Biodivers Conserv 19: 317-28.

Sondaar PY. 1977. Insularity and its effects on mammal evolution. In: Hecht MK, Goody PC, Hecht BM, eds: Major patterns in vertebrate evolution, New York: Plenum Press, 671–707.

Stamps JA, Buechner M. 1985. The territorial defense hypothesis and the ecology of insular vertebrates. Quart R Biol 60: 155-81.

Swift JA, Roberts P, Boivin N, Kirch PV. 2018. Restructuring of nutrient flows in island ecosystems following human colonization evidenced by isotopic analysis of commensal rats. Proc Natl Acad Sci 115: 6392.

Symonds MR, Blomberg SP. 2014. A primer on phylogenetic generalised least squares. In: Garamszegi, LZ, ed: Modern phylogenetic comparative methods and their application in evolutionary biology, Berlin: Springer, 105-130.

Tate ML, Adamson JR, Tami AE, Bauer TW. 2004. The osteocyte. Int J Biochem Cell Biol 36: 1-8.

Taylor R. 1990. Interpretation of the correlation coefficient: a basic review. J. Diagnost. Med. Sonogr 6: 35-9.

Towns DR, Atkinson IA, Daugherty CH. 2006. Have the harmful effects of introduced rats on islands been exaggerated? Biol Invasions 8: 863-891.

van der Geer AA. 2018. Changing invaders: trends of gigantism in insular introduced rats. Environ Conserv 45: 203-211.

van der Geer AA. 2019. Effect of isolation on coat colour polymorphism of Polynesian rats in Island Southeast Asia and the Pacific. PeerJ 7: e6894.

van der Geer AA, Lyras GA, Lomolino MV, Palombo MR, Sax DF. 2013. Body size evolution of palaeo-insular mammals: temporal variations and interspecific interactions. J Biogeogr 40: 1440-1450.

Van Valen LM. 1973. Patterns and the balance of nature. Evol Theor, 1: 31-49.

van den Hoek Ostende LW, van der Geer AA, Wijngaarden CL. 2017. Why are there no giants at the dwarves feet? Insular micromammals in the eastern Mediterranean. Quatern Int 445: 269-278.

Ventura J, Fuster MJ. 2000. Morphometric analysis of the black rat, *Rattus rattus*, from Congreso Island (Chafarinas Archipielago, Spain). Orsis: organismes i sistemes 15: 91-102.

Whittaker RJ, Fernández-Palacios JM. 2007. Island biogeography: ecology, evolution, and conservation. Oxford: University Press.

Yabe T. 1994. Fat deposits for wintering in the Norway rat, *Rattus norvegicus*. J Mammal Soc Japan 19: 129-133.

Yom-Tov Y, Yom-Tov S, Moller H. 1999. Competition, coexistence, and adaptation amongst rodent invaders to Pacific and New Zealand islands. J Biogeog 26: 947-58.

Zafonte F, Masini F. 1992. Enamel structure evolution in the first lower molar of the endemic murids of the genus *Microtia* (Pliocene, Gargano, Italy). Boll Soc Paleontol Ital 31: 335-349.

FIGURE CAPTIONS

Figure 1.

The specimens examined in the present study (all caudal view) showing the size gradient in the sample and midshaft sampling location (dashed line, 1A), a histological cross-section through one of the specimens and an associated region of interest examined for osteocyte lacunae (1B), and examples of more (left) and less (right) widely dispersed osteocyte lacunae in a giant and small femora respectively (1C).

Figure 2.

Estimated body weight in grams (top), and femur midshaft measurements in medial-lateral and cranial-caudal planes in mm (bottom) for the Timor specimens (highlighted on the graph by the boxes) presented amongst other 17 known weight Asia-Pacific murine rodents.

Figure 3.

Negative allometric relationships between log estimated body mass (top row), log cranial-caudal (middle row) and log medial-lateral midshaft (bottom row) diameter data, and log osteocyte lacunae (including data corrected by midshaft size, Y axis) in the sample. Regression line is red and the confidence interval is indicted by blue lines.

Table 1. Raw data for the entire sample reporting histology and gross morphometric femoral measurements in this study: MAXL - maximum intact femur length in mm, FHDM - femoral head diameter in mm, MLW - medial-lateral midshaft femur width in mm, CCD - cranial-caudal midshaft femur depth in mm, Ot.N (a) – osteocyte lacunae number, Ot.Dn – osteocyte lacunae number (a) divided by section area (b) in mm^2. *Data from Miszkiewicz et al., 2019

Femur accession ID (Australian National University)	**MAXL**	**FHDM**	**MLW**	**CCD**	**Ot.N (a)**	**Section area (b)**	**Ot.Dn (a/b)**
TDD 1 #1	n/a	n/a	7.18	5.24	2778	0.929	2990.31
TDD 1 #2	n/a	n/a	6.84	5.39	2380	0.927	2567.42
TDD 1 #3	n/a	n/a	7.25	5.89	2292	0.923	2483.21
TDS 0-30 #4	n/a	n/a	6.15*	4.87*	2569	0.844	3043.84
TDS 15-30 #6	n/a	n/a	3.59	2.31	877	0.346	2534.68
TDD 1 #7	n/a	n/a	4.18	3.02	1628	0.580	2806.90
TDD 1 #8	26.27	2.41	3.21	2.61	1218	0.375	3248.00
TDD 1 #9	29.73	3.51	3.85	2.5	1996	0.586	3406.14
TDD 1 #10	26.13	2.78	3.13	2.57	2287	0.581	3936.32
TDD 1 #11	n/a	n/a	2.33*	1.98*	1579	0.452	3493.36

Table 2. Raw data for individuals of 17 Asia-Pacific murine species of known weight and femoral midshaft size, along with the fossil specimens examined in the present study. The specimens were studied by Ken Aplin and are registered at the Commonwealth Scientific and Industrial Research Organisation (CSIRO, Australia). KMH refer to field number identifications and the two KMH specimens are reposited at Bogor Zoology Museum (Bogor, Indonesia). We use these data for illustrative purposes only (see Fig. 1). Where data were collected for more than one individual per species, the Weight, MLW, and CCD are means. Estimated body mass for the Timor fossil murines is based on a PGLS regression accounting for uncertainty in phylogenetic relationships and divergence times reported in text. *Data from Miszkiewicz et al., 2019.

Taxon/ subfamily	Comparative significance	Institution	Accession ID	Weight (g)	MLW (mm)	CCD (mm)
Parahydromys asper	Asian native - waterside rat of New Guinea	CSIRO	#15689	470	4.99	3.47
Crossomys moncktoni	Asian native - earless water rat of New Guinea	CSIRO	#15679, #15678	230 (240, 220)	3.90 (3.88, 3.92)	2.84 (2.85, 2.83)
Pseudomys fumeus	Southeast Australian native - smoky mouse of Australia	CSIRO	#13231	63	1.92	1.55
Conilurus penicillatus	Australasian native - Brush-tailed rabbit rat of Australia	CSIRO	#1007, #1009	107 (111, 103)	3.02 (2.97, 3.06)	2.77 (2.83, 2.71)
Abeomelomys sevia	Asian native - highland brush mouse of Papua New Guinea	CSIRO	#15693, #15694	(59.5) 64, 55	2.105 (2.33, 1.88)	1.56 (1.57, 1.54)
Xeromys myoides	Australasian native - false water rat of Australia and Papua New Guinea	CSIRO	#10022	44.5	2.42	1.62
Hydromys habbema	Asia native - mountain water rat of West Papua, Indonesia, and Papua New Guinea	CSIRO	#15691	68	2.66	1.95

Mallomys istapantap	Asian native - subalpine woolly rat of West Papua, Indonesia, and Papua New Guinea	CSIRO	#15681	1200	8.49	5.8
Rattus fuscipes	Australasian native – bush rat of Australia	CSIRO	#17928, #17927, #17922, #17201	126.75 (110, 150, 133, 114)	2.67 (2.65, 3.03, 2.71, 2.27)	2.13 (2.15, 2.28, 2.17, 1.91)
Rattus lutreolus	Australasian native – swamp rat of Australia	CSIRO	#6806	129	3.13	2.06
Mus domesticus	House mouse – included as a domesticated small rodent reference	CSIRO	#8624, #18846, #19463	14 (10, 14, 18)	1.41 (1.4, 1.33, 1.5)	1.17 (1.18, 1.18, 1.14)
Paramelomys levipes	Asian native - long-nosed mosaic-tailed rat or Papua New Guinea	CSIRO	#15695	44	1.64	1.46
Pogonomys loriae	Asian native - tree mouse of Australia, Indonesia, and Papua New Guinea.	CSIRO	#16516	62	2.19	1.95
Protochromys fellowsi	Asian native - red-bellied mosaic-tailed rat of Papua New Guinea	CSIRO	#16504	98	2.73	1.85
Melomys burtoni	Australasian native - grassland mosaic-tailed rat of Australia and Papua New Guinea	CSIRO	#3673	40	1.79	1.74
Mammelomys sp.	Asian native - rodent genus endemic to New Guinea	KMH	#1893	116	2.72	2.6
Rattus praetor	Asian native - large spiny rat of Papua New Guinea, and the Solomon Islands	KMH	#1833	435	4.81	3.49
Murinae spp.	Asian material used in this study	ANU	TDD 1 #1	1015	7.18	5.24
Murinae spp.		ANU	TDD 1 #2	990	6.84	5.39
Murinae spp.		ANU	TDD 1 #3	1188	7.25	5.89
Murinae spp.		ANU	TDS 0-30 #4	765	6.15*	4.87*
Murinae spp.		ANU	TDS 15-30 #6	156	3.59	2.31
Murinae spp.		ANU	TDD 1 #7	262	4.18	3.02

Murinae spp.		ANU	TDD 1 #8	158	3.21	2.61
Murinae spp.		ANU	TDD 1 #9	187	3.85	2.5
Murinae spp.		ANU	TDD 1 #10	150	3.13	2.57
Murinae spp.		ANU	TDD 1 #11	75	2.33*	1.98*

Table 3. Data for the entire murine sample representing femoral morphometric and histological measurements: N – sample size, MIN. = minimum value of data, MAX. – maximum value of data, SD – standard deviation.

VARIABLES	N	MIN.	MAX.	MEAN	SD
MAXL	3	26.13	29.73	27.38	2.04
FHDM	3	2.41	3.51	2.90	0.56
MLW	10	2.33	7.25	4.77	1.88
CCD	10	1.98	5.89	3.64	1.51
Ot.N (#)	10	877.00	2778.00	1960.40	615.87
Section area (mm^2)	10	0.35	0.93	0.65	0.23
Ot.Dn (#/mm^2)	10	2483.21	3936.32	3051.02	474.99
Ot.Dn/ MLW	10	342.51	1499.30	766.03	393.57
Ot.Dn/ CCD	10	421.60	1764.32	1002.32	472.12

Table 4. Spearman's *Rho* correlations and ordinary least squares (OLS) regressions assessing relationships between osteocyte lacunae and rat femur size and estimated body mass (using raw and log transformed data respectively): coefficient of determination (r^2), slope (*b*), confidence interval (CI), intercept (*Y*), Total sample size is 10 in each test. *statistically significant at $p < 0.05$; †statistically significant at Bonferroni corrected $p < 0.017$.

X axis	Y axis	*Rho*	*p*
estimated body mass (g)	Ot.Dn (#/mm^2)	-0.661	<0.038*
	Ot.Dn/CCD	-0.939	<0.0001*†
	Ot.Dn/MLW	-0.952	<0.0001*†
CCD (mm)	Ot.Dn (#/mm^2)	-0.576	0.082
	Ot.Dn/CCD	-0.915	<0.0001*†
	Ot.Dn/MLW	-0.891	0.001*†
MLW (mm)	Ot.Dn (#/mm^2)	-0.721	0.019*
	Ot.Dn/CCD	-0.952	<0.0001*†
	Ot.Dn/MLW	-0.976	<0.0001*†
OLS X axis	**Y axis**	***r*^{2}, *b*, *Y*, CI**	***p***
log estimated body mass	log Ot.Dn	0.367, -0.092, 8.546, -0.178 -0.024	0.064
	log Ot.Dn/CCD	0.952, -0.498, 9.678, -0.568 -0.429	<0.0001*†
	log Ot.Dn/MLW	0.917, -0.491, 9.361, -0.560 -0.418	<0.0001*†
log CCD	log Ot.Dn	0.317, -0.210, 8.268, -0.415 -0.028	0.090
	log Ot.Dn/CCD	0.940, -1.211, 8.269, -1.436 -1.036	<0.0001*†
	log Ot.Dn/MLW	0.864, -1.167, 7.94, -1.486 -0.920	<0.0001*†
log MLW	log Ot.Dn	0.409, -0.243, 8.376, -0.436 -0.069	0.046*
	log Ot.Dn/CCD	0.937, -1.233, 8.637, -1.432 -0.965	<0.0001*†
	log Ot.Dn/MLW	0.947, -1.244, 8.378, -1.432 -1.058	<0.0001*†

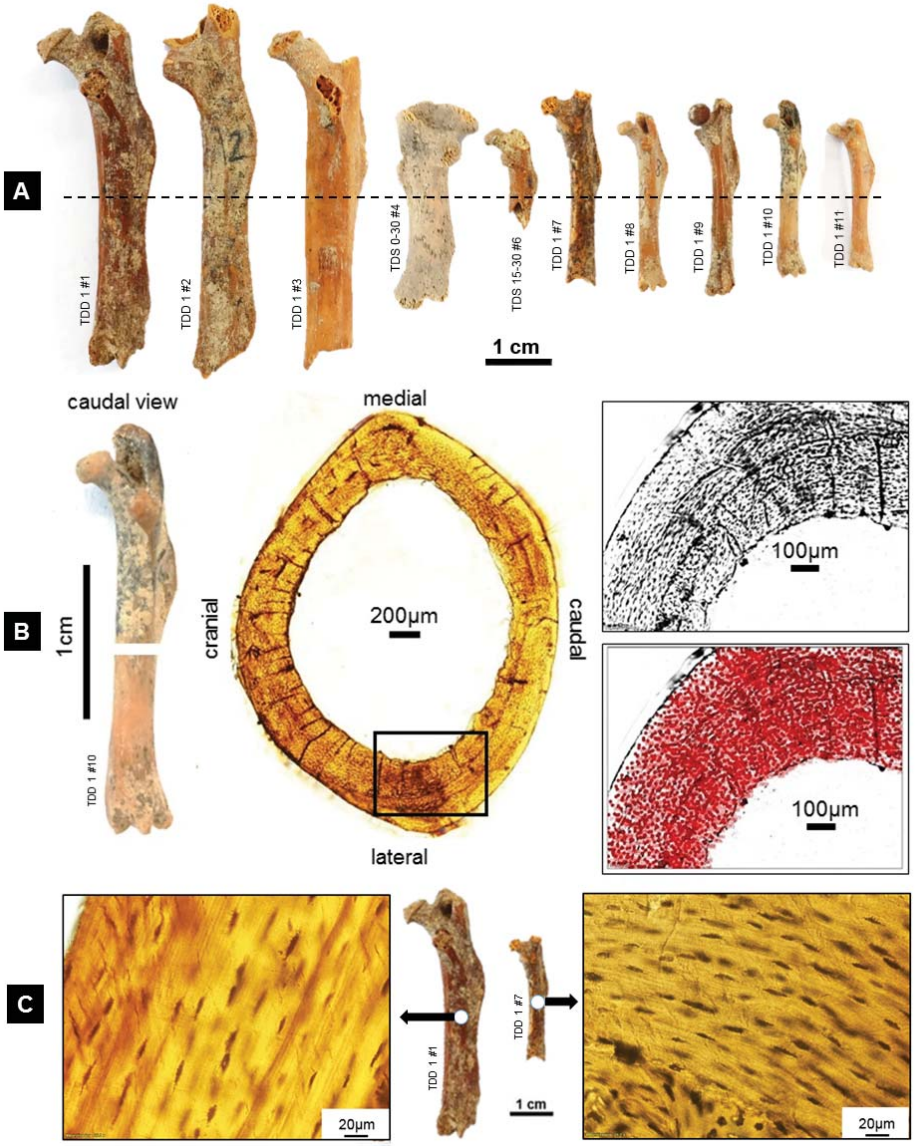

Figure 1.

The specimens examined in the present study (all caudal view) showing the size gradient in the sample and midshaft sampling location (dashed line, 1A), a histological cross-section through one of the specimens and an associated region of interest examined for osteocyte lacunae (1B), and examples of more (left) and less (right) widely dispersed osteocyte lacunae in a giant and small femora respectively (1C).

250x310mm (96 x 96 DPI)

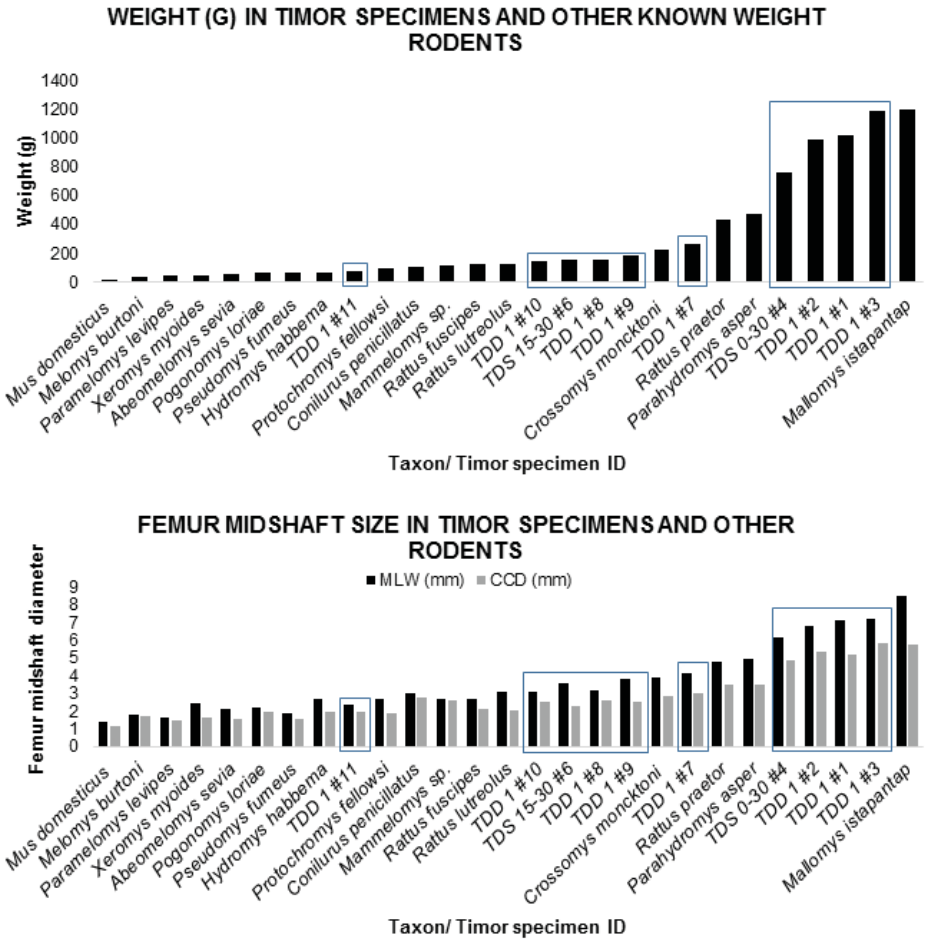

Figure 2.

Estimated body weight in grams (top), and femur midshaft measurements in medial-lateral and cranial-caudal planes in mm (bottom) for the Timor specimens (highlighted on the graph by the boxes) presented amongst other 17 known weight Asia-Pacific murine rodents.

179x175mm (96 x 96 DPI)

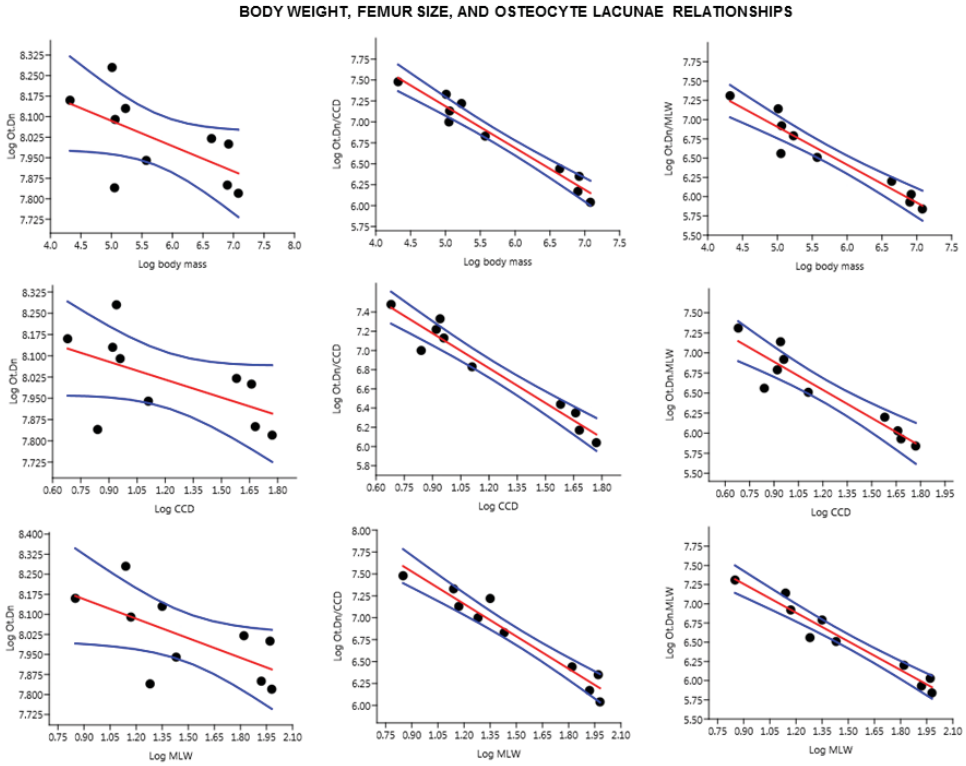

Figure 3.

Negative allometric relationships between log estimated body mass (top row), log cranial-caudal (middle row) and log medial-lateral midshaft (bottom row) diameter data, and log osteocyte lacunae (including data corrected by midshaft size, Y axis) in the sample. Regression line is red and the confidence interval is indicted by blue lines.

236x187mm (96 x 96 DPI)